Bioconjugate Chemistry

Technical Note

pubs.acs.org/bc

[^{18}F]Fluoromethyl-PBR28 as a Potential Radiotracer for TSPO: Preclinical Comparison with [^{11}C]PBR28 in a Rat Model of Neuroinflammation

Byung Seok Moon,[†] Bom Sahn Kim,[‡] Chansoo Park,[§] Jae Ho Jung,[†] Youn Woo Lee,[†] Ho-Young Lee,[†] Dae Yoon Chi,*[,§] Byung Chul Lee,*[,†,∥] and Sang Eun Kim*[,†,∥,#]

[†]Department of Nuclear Medicine, Seoul National University Bundang Hospital, Seoul National University College of Medicine, Seoul, Korea

[‡]Department of Nuclear Medicine, Ewha Womans University Medical Center, Seoul, Korea

[§]Department of Chemistry, Sogang University, Seoul, Korea

[∥]Advanced Institutes of Convergence Technology, Suwon, Korea

[#]Department of Transdisciplinary Studies, Graduate School of Convergence Science and Technology, Seoul National University, Seoul, Korea

Supporting Information

ABSTRACT: To develop radiotracer for the translocator protein 18 kDa (TSPO) in vivo, *N*-(2-[^{18}F]fluoromethoxybenzyl)-*N*-(4-phenoxypyridin-3-yl)-acetamide ([^{18}F]**1**, [^{18}F]fluoromethyl-PBR28) was prepared by incorporating of fluorine-18 into triazolium triflate-PBR28 precursor (**7**). The radiochemical yield of [^{18}F]**1** after HPLC purification was 35.8 ± 3.2% (n = 11, decay corrected). Radiotracer [^{18}F]**1** was found to be chemically stable when incubated in human serum for 4 h at 37 °C. Both aryloxyanilide analogs (**1** and **2**) behaved similarly in terms of lipophilicity and in vitro affinity for TSPO. Here, both radiotracers were directly compared in the same inflammatory rat to determine whether either radiotracer provides more promising in vivo TSPO binding. Uptake of [^{18}F]**1** in the inflammatory lesion was comparable to that of [^{11}C]PBR28, and [^{18}F]**1** rapidly approached the highest target-to-background ratio at early imaging time (35 min postinjection versus 85 min postinjection for [^{11}C]PBR28). These results suggest that [^{18}F]**1** is a promising radiotracer for imaging acute neuroinflammation in rat. In addition, our use of a triazolium triflate precursor for [^{18}F]fluoromethyl ether group provides the convenient application for radiofluorination of radiotracer containing a methoxy group.

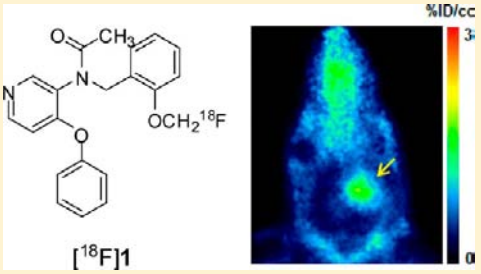

INTRODUCTION

The expression of a translocator protein (18 kDa; TSPO), which was formerly named the peripheral benzodiazepine receptor (PBR), is a reliable hallmark of microglial activation in neuroinflammatory diseases.[1,2] Several studies reported that increased TSPO density has been used as an indicator of neuronal damage or loss in neuroinflammatory diseases, such as Alzheimer's disease, Huntington's disease, multiple sclerosis, and ischemic brain injury.[3−6] Therefore, successful development of a TSPO specific positron emission tomography (PET) radiotracers will help the clinical demand to monitor progression of neuroinflammation or measure therapeutic efficacy. (*R*)-*N*-Methyl-*N*-(1-methylpropyl)-1-(2-chlorophenyl)isoquinoline-3-carboxamide ([^{11}C]-(*R*)-PK11195), as one of the first developed TSPO PET ligands, has been used in most of the PET imaging for neuroinflammatory studies over the past few decades.[7] However, [^{11}C]-(*R*)-PK11195 has several limitations, i.e., a high level of nonspecific binding and a low signal-to-noise ratio.[8] A previous study in a nonhuman primate brain reported that approximately 50% of the [^{11}C]-(*R*)-PK11195 uptake was nonspecific.[9] PET studies of *N*-5-fluoro-2-phenoxyphenyl)-*N*-(2,5-dimethoxybenzyl)acetamide ([^{11}C]DAA1106) also showed a low TSPO specific signal in small animals.[10,11] Therefore, a number of alternative TSPO PET radioligands for neuroinflammatory imaging have been developed over the last several years.[12] Among them, *N*-acetyl-*N*-(2-[^{11}C]methoxybenzyl)-2-phenoxy-5-pyridinamine ([^{11}C]PBR28, [^{11}C]**2**), a close analogue of DAA1106, was developed for the imaging of neuroinflammation.[13] [^{11}C]PBR28 exhibited a high specific signal to TSPO greater than that of [^{11}C]PK11195 or [^{11}C]DAA1106 in the nonhuman primate brain study and had adequate sensitivity to localize and quantify the expression of TSPO in a neuroinflammatory rat model.[6,12] However, the use of [^{11}C]PBR28 limits the clinical use of [^{11}C]PBR28 due to the short half-life of carbon-11 ($t_{1/2}$ = 20.38 min), whereas

Received: December 3, 2013
Revised: January 7, 2014
Published: January 8, 2014

fluorine-18 has advantages over carbon-11 if a dynamic PET experiment has a turnover time longer than 100 min. Fluorine-18 also has a lower positron energy (650 keV versus 960 keV), and ^{18}F-labeled ligands produce higher quality images with a higher spatial resolution in PET measurements. In addition, fluorine-18 is convenient for long-term storage and long-distance transportation to other facilities. In this work, we designed [^{18}F]fluoromethyl-PBR28 (*N*-acetyl-*N*-(2-[^{18}F]-fluoromethoxybenzyl)-2-phenoxy-5-pyridinamine, [^{18}F]**1**) as a derivative of PBR28 containing a [^{18}F]fluoromethyl moiety (−CH_2[^{18}F]F) (Figure 1). The [^{18}F]fluoromethyl moiety on

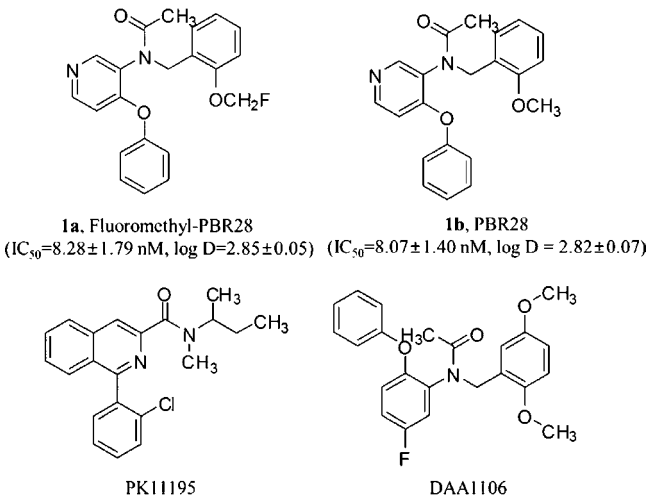

Figure 1. Structure of various TSPO PET ligands.

PBR28 is sterically almost identical to −[^{11}C]CH_3, which exhibits promising results for TSPO imaging by PET, indicating that the biological properties of [^{11}C]PBR28 could be maintained. Although an aryl [^{18}F]fluoromethoxy group was more attractive than others for replacement of the [^{11}C]-methoxy group by general methods, the radiochemical yield was relatively low as a result of the multistep labeling procedure or volatility of the prosthetic groups such as [^{18}F]FCH_2Br, [^{18}F]FCH_2I, and [^{18}F]FCH_2OTf, leading to a relatively low specific activity and long synthetic time.[14−16] Therefore, in the present study, we adapt novel the radiofluorination method of the [^{18}F]fluoromethyl group using triazolium triflate that was recently developed by us[17] and describe the details of an efficient single-step radiofluorination from triazolium triflate-PBR28 precursor **7** (Scheme 1), which could overcome the disadvantages described above. In addition, we propose the application of the newly developed TSPO PET radioligand, [^{18}F]**1**, and evaluate its suitability as an indirect hallmark of neuroinflammatory diseases.

MATERIALS AND METHODS

Chemistry and Radiochemistry. All commercial reagents and solvents were used without further purification unless otherwise specified. Reagents and solvents were commercially purchased from Sigma-Aldrich (U.S.A.). All reaction was monitored by thin-layer chromatography (TLC), unless otherwise noted. TLCs were performed on Merck silica gel glass plates (60 F_{254}). Visualization was accomplished by irradiation with a UV lamp. Flash column chromatography was performed with silica gel (Merck, 230−400 mesh, ASTM). ^{1}H and ^{13}C NMR spectra were recorded on a INOVA-400 (400 MHz), and INOVA-500 (500 MHz) spectrometer at ambient temperature. Chemical shifts were reported in parts per million (ppm, δ units). Melting points (m.p.) are recorded using a Krüss melting point apparatus. Mass spectra (FAB) were obtained using a Jeol JMS700 high-resolution mass spectrometer at the Korea Basic Science Center, Daegu, Korea. $H_2{}^{18}O$ was purchased from Taiyo Nippon Sanso Corporation (Japan). ^{18}F-Fluoride was produced at Seoul National University Bundang Hospital by ^{18}O(p,n)^{18}F reaction through proton irradiation using a KOTRON-13 cyclotron (Samyoung Unitech Co., Ltd.). C18 plus Sep-Pak cartridges were purchased from Waters Corp. (U.S.A.). HPLC purification was performed with a Gilson 322 (Waters, Semi-Preparative Xterra RP-18, 10 μm, 10 × 250 mm). The purified radiotracer and authentic compound were analyzed using Thermo Separation Products System (U.S.A.) (YMC, analytical YMC-triart C18, 5 μm, 4.6 × 250 mm) equipped with a NaI radiodetector (Raytest) and a UV-detector. HPLC-grade solvents (J. T. Baker, U.S.A.) were used for HPLC purification after membrane filtering (Whatman, 0.22 μm). Radio-TLC was analyzed on a Bioscan radio-TLC scanner (U.S.A.). All radioactivities were measured using a VDC-505 activity calibrator from Veenstra Instruments (Netherlands). PBR28 and desmethyl-PBR28 were persuaded from Huayi Isotopes Company (China). [^{11}C]PBR28 was synthesized from desmethyl PBR28 (**6**) and [^{11}C]CH_3OTf using a TRACERlab FX C pro module (GE Healthcare).

1-(Chloromethyl)-3-methyl-4-phenyl-1*H*-1,2,3-triazol-3-ium triflate (5).[18] A mixture of aqueous 37% formaldehyde (50 mL, 654 mmol), glacial acetic acid (5.6 mL, 98.4 mmol), and 1,4-dioxane (50 mL) was stirred for 15 min at 25 °C and was treated with NaN_3 (6.4 g 98.4 mmol) and phenylacetylene (7.2 mL, 65.4 mmol). Resulting mixture was stirred for 10 min and treated with sodium ascorbate (2.5 g, 12.6 mmol) and a solution of $CuSO_4{\cdot}5H_2O$ (2.5 g, 12.6 mmol) in water (4 mL).

Scheme 1[a]

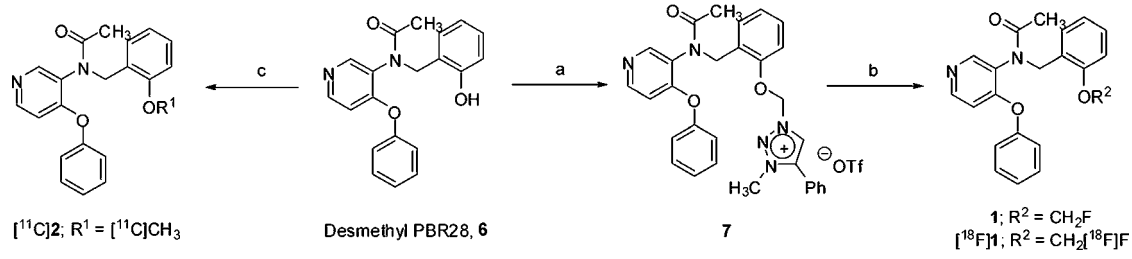

[a]Reaction conditions: (a) 1-(Chloromethyl)-3-methyl-4-phenyl-1*H*-1,2,3-triazol-3-ium triflate (**5**), *tert*-BuOK, DMF, r.t., 5 h; (b) TBAF-$3H_2O$, CH_3CN, 80 °C, 1 h for **1** or TBA[^{18}F]F complex, *tert*-BuOH, 120 °C, 10 min for [^{18}F]**1**; (c) [^{11}C]CH_3OTf, acetone, 80 °C, 5 min.

dx.doi.org/10.1021/bc400556h | *Bioconjugate Chem.* 2014, 25, 442−450

The resulting mixture was stirred for 18 h at 25 °C and filtered through a pad of Celite. Filtrate was diluted with water (300 mL) and extracted with CH_2Cl_2 (3 × 50 mL). Combined organic extracts were dried over Na_2SO_4 and concentrated under reduced pressure to afford a mixture of hydroxymethyl triazoles as yellow solid which was used in the next step without purification. To the mixture of crude (1.02 g, 5.82 mmol), $SOCl_2$ (3.2 mL, 43.7 mmol) was added at 0 °C and reaction mixture was stirred at 25 °C for overnight. The reaction mixture was concentrated under reduced pressure, and residue was purified with flash chromatography (EtOAc/hexane = 20/80) to afford a 1-chloromethyl-4-phenyl-1*H*-1,2,3-triazole as a white solid (237 mg, 21%): mp 118−120 °C; ^{1}H NMR (500 MHz, $CDCl_3$) δ 7.98 (s, 1H), 7.83 (d, J = 7.0 Hz, 2H), 7.44 (t, J = 7.5 Hz, 2H), 7.38−7.35 (m, 1H), 6.08 (s, 2H); ^{13}C NMR (125 MHz, $CDCl_3$) δ 149.3, 129.9, 129.1, 128.9, 126.1, 119.8, 54.8 (CAS Registry Number: 1043553−26−9). A solution of 1-(chloromethyl)-4-phenyl-1*H*-1,2,3-triazole (387 mg, 2.0 mmol) in acetonitrile (4 mL) at 25 °C was treated with methyl triflate (329 μL, 3.0 mmol). The reaction mixture was stirred at room temperature for 1 h. After concentrated under reduced pressure, the crude product was purified with flash column chromatography (MeOH/CH_2Cl_2 = 5/95) to obtain the product as a white solid (710 mg, 99%): mp 107−109 °C; ^{1}H NMR (500 MHz, $CDCl_3$) δ 8.94 (s, 1H), 7.64−7.56 (m, 5H), 6.29 (s, 2H), 4.29 (s, 3H); ^{13}C NMR (125 MHz, $CDCl_3$) δ 144.2, 132.4, 130.0, 129.7, 129.5, 121.5, 120.6 (q, J = 318 Hz), 57.2, 39.2. HRMS (FAB) m/z calcd. for $[C_{11}H_{11}ClF_3N_3O_3S$ - OTf$]^+$: 208.0642; found: 208.0639.

1-[2-(*N*-Acetyl-*N*-4-phenoxypyridin-3-ylaminomethyl)phenoxymethyl]-3-methyl-4-phenyl-1*H*-1,2,3-triazol-3-ium triflate (7). A solution of desmethyl PBR28 (**6**, 333 mg, 1.0 mmol) in DMF (4 mL) at 0 °C was treated with ^{t}BuOK (224 mg, 2.0 mmol) and 1-(chloromethyl)-3-methyl-4-phenyl-1*H*-1,2,3-triazol-3-ium triflate (360 mg, 1.0 mmol).[19] The reaction mixture was stirred for 5 h at room temperature and quenched with water (100 mL), and resulting mixture was extracted with EtOAc (30 mL). Combined organic fraction was washed with saturated Na_2SO_3 solution (100 mL), dried Na_2SO_4, and evaporated under reduced pressure. The crude product was purified with flash chromatography column (MeOH/CH_2Cl_2 = 5/95) to obtain the product as a pale yellow semisolid (230 mg, 35%): ^{1}H NMR (500 MHz, $CDCl_3$) δ 8.71 (s, 1H), 8.27−8.26 (m, 2H), 7.66−7.56 (m, 5H), 7.41 (t, J = 8.0 Hz, 2H), 7.35−7.32 (m, 1H), 7.28−7.25 (m, 2H), 7.15 (d, J = 8.0 Hz, 1H), 7.03 (t, J = 7.5 Hz, 1H), 6.81 (d, J = 8.0 Hz, 2H), 6.56 (d, J = 5.5 Hz, 1H), 6.46 (s, 2H), 4.94 (dd, J = 84.0, 14.5 Hz, 2H), 4.28 (s, 3H), 1.96 (s, 3H); ^{13}C NMR (125 MHz, $CDCl_3$) δ 170.6, 160.7, 153.5, 152.8, 151.2, 151.0, 143.8, 132.1, 131.6, 130.5, 129.9, 129.8, 129.6, 128.8, 128.4, 126.4, 126.3, 124.1, 121.6, 120.5, 113.9, 110.7, 79.7, 46.5, 38.7, 22.2; HRMS (FAB) m/z calcd. for $[C_{31}H_{28}F_3N_5O_6S$ - OTf$]^+$: 506.2192; found: 506.2195.

***N*-Acetyl-*N*-(2-fluoromethoxybenzyl)-2-phenoxy-5-pyridinamine (1).** A stirred mixture of triazolium triflate salt precursor (7, 32 mg, 0.05 mmol) and TBAF (20 mg, 0.075 mmol) in CH_3CN (0.5 mL) was stirred at 80 °C for 1 h. The reaction mixture was quenched with water (30 mL), and resulting mixture was extracted with CH_2Cl_2 (30 mL). Combined organic fraction were washed with brine (20 mL) and dried over Na_2SO_4. After concentrated under reduced pressure, the crude product was purified with flash chromatography (EtOAc/hexane = 50/50) to obtained the product as a white semi solid (**1**, 15 mg, 83%): ^{1}H NMR (500 MHz, $CDCl_3$) δ 8.30 (d, J = 5.6 Hz, 1H), 8.23 (s, 1H), 7.41(t, J = 7.8 Hz, 3H), 7.29−7.23 (m, 3H), 7.05−7.00 (m, 2H), 6.86 (d, J = 8.4 Hz, 1H), 6.56 (d, J = 5.2 Hz, 1H), 5.45 (ddd, J = 54.8, 17.6, 2.4 Hz, 2H), 5.05 (dd, J = 51.6, 14.4 Hz, 2H), 2.00 (s, 3H); ^{13}C NMR (125 MHz, $CDCl_3$) δ 170.9, 161.0, 155.24, 155.22, 153.3, 151.8, 151.0, 131.8, 130.6, 129.5, 126.4, 126.2, 123.8, 120.9, 114.9, 110.7, 100.8 (d, J = 218 Hz), 46.1, 22.4; HRMS (FAB) m/z calcd. for $[C_{21}H_{19}FN_2O_3$ + H$]^+$: 367.1458; found: 367.1456.

***N*-Acetyl-*N*-(2-[^{18}F]fluoromethoxybenzyl)-2-phenoxy-5-pyridinamine ([^{18}F]1).** The radiotracer, [^{18}F]fluoromethyl-PBR28, was prepared by nucleophilic aliphatic substitution on the triazolium triflate-PBR28 (**7**) precursor with fluorine-18 in a single-step radiolabeling procedure. Briefly, ^{18}F was prepared by the ^{18}O(p,n)^{18}F reaction using $H_2{}^{18}O$ as the target material. [^{18}F]F^-/$H_2{}^{18}O$ was isolated from the enriched water by trapping in a Chromafix-HCO_3 cartridge, previously activated with 2 mL of ethanol and then washed 5 mL of water, and then eluting with methanol:water (1:0.2 mL) dissolved 40% $TBAHCO_3$ (0.8 equiv). This solution was dried by azeotropic distillation with acetonitrile (0.3 mL) under nitrogen stream (×2) and, subsequently, triazolium triflate-PBR28 precursor **7** (2.3 or 4.5 mg) in various solvent (0.4 mL) such as CH_3CN, DMF, *tert*-butanol, or *tert*-butanol:CH_3CN mixture (4:1) was added. The reaction mixture was heated at desired temperature for 10 or 15 min. After the mixture was cooled to room temperature, the reaction mixture was diluted with 10 mL of water. This solution was loaded into a tC18 Sep-Pak cartridge, washed with 10 mL of water, and eluted with 1.5 mL of CH_3CN. The combined solution was separated by a semiprep HPLC system (Waters, Xterra RP-18, 10 × 250 mm, 10 μm) using a UV detector at 254 nm and a gamma-ray detector. Acetonitrile and water (45:55) were used as a mobile phase at a flow rate of 3 mL/min. The product fraction was collected after approximately 13.5 min (Figure S1). The fraction of [^{18}F]-fluoromethyl-PBR28 collected from the HPLC system was diluted with 20 mL of water. The diluted solution was exchanged to 5% EtOH/saline solution by a tC18 Sep-Pak cartridge to remove the clinically unavailable HPLC solvent. The identity was confirmed by coinjection with authentic compound using analytical HPLC system (YMC pro triart, 4.6 × 250 mm, 5 μm) (Figure S2).

***N*-Acetyl-*N*-(2-[^{11}C]methoxybenzyl)-2-phenoxy-5-pyridinamine ([^{11}C]2).** [^{11}C]PBR28 was synthesized from desmethyl PBR28 (**6**) and purified by reverse-phase HPLC (Figure S3) using a TRACERlab FX C pro module according to the literature with little modification.[20−22]

Log *D* Determination. The log *D* value was measured four times by mixing a solution of [^{18}F]fluoromethyl-PBR28 (approximately 0.74 MBq) or [^{11}C]PBR28 (approximately 1.5 MBq) in 5% ethanol:saline (10 μL) with sodium phosphate buffer (0.15 M, pH 7.4, 5.0 mL) and *n*-octanol (5.0 mL) in a test tube. After vortexing for 1 min, each tube was then stored for 3 min at room temperature and the phases were separated. Samples of each phase (100 μL) were counted for radioactivity. Log *D* is expressed as the logarithm of the ratio of the counts from *n*-octanol versus that of the sodium phosphate buffer.

In Vitro TSPO Binding Affinity. Leukocytes were isolated from 50 mL of heparinized whole blood by Ficoll-Hypaque density centrifugation using a Lymphocyte Separation Medium (Lonza, Walkersville, MD, U.S.A.) according to the manufacturer's instructions. Following isolation, these leukocytes were

viably cryopreserved. Prior to the day of the assay, the cells were thawed, diluted with an equal volume of buffer (50 mM HEPES, pH 7.4), homogenized with a Teflon pestle, and centrifuged at 20 000*g* for 15 min at 4 °C. The resulting crude membrane pellet was resuspended in 2.4 mL buffer and stored at −70 °C. The protein concentration was determined using the Bradford Protein Assay (Bio-Rad, Hercules, CA, U.S.A.). For the binding assay, leukocytes (100 mL resuspended membranes) were added to the mixture containing 100 μL of radioligand ([^{3}H]PK11195, Specific radioactivity: 3.08 GBq/μmol, IC_{50} = 1.40 ± 0.4 nM)[23] and 10% ethanol in a final volume of 1 mL for the saturation studies. For the inhibition studies, 1 mL of the reaction mixture containing 50 μL of fluoromethyl-PBR28 or PBR28 (0.124−10 000 nM in 10% ethanol) and 0.07 nM [^{3}H]PK11195 in 10% ethanol was incubated for 30 min at room temperature for the binding assay. The reaction mixture was filtered through Whatman GF/A glass filters and washed twice with 3 mL of 10% ethanol aliquots. The radioactivity retained on the filter was determined by a β-counter. Under the assay conditions, the percent of the specific binding fraction was less than 20% of the total ^{3}H radioactivity. The results of the inhibition and saturation experiments were subjected to nonlinear regression analysis using PRISM software to calculate the IC_{50} values of fluoromethyl-PBR28 and PBR28.

Stability of [^{18}F]Fluoromethyl-PBR28 in Human Serum. The stability of [^{18}F]fluoromethyl-PBR28 was assayed by monitoring the Radio-TLC profile and determining its radiochemical purity. To determine the in vitro serum stability, 100 μL of [^{18}F]fluoromethyl-PBR28 in 5% EtOH/saline was incubated with 0.5 mL of human serum at 37 °C for 4 h, and the solution was analyzed at 0, 10, 30, 60, 120, and 240 min by a radio-TLC scanner using MeOH−CH_2Cl_2 (10:90) as the developing solvent.

LPS-Induced Neuroinflammatory Rat Model. Male Sprague−Dawley rats weighing 200−250 g were used as the neuroinflammatory brain model using lipopolysaccharide (LPS; Sigma-Aldrich, St. Louis, MO, U.S.A.). The rats were anesthetized with Ketamine HCL (50 mg/kg; Zoletil 50, Virbac, Carros, France) and Xylazine HCl (0.2 mg/kg; Rumpen, Bayer Korea, Seoul, Korea) and placed on a stereotactic apparatus to immobilize the head. The skull was exposed, and a small hole was punctured with the use of a bone drill. Next, 50 μg of LPS was infused into the right striatum through the use of a Hamilton syringe at a flow rate of 0.5 μL/min (AP, 0.8 mm; L, −2.7 mm and P, −5.0 mm from the bregma).[24] The Hamilton syringe was sustained in place for 10 min to avoid backflow of LPS. The small hole in the skull was filled with wax, and the incised scalp was sutured. All of the animal experiments were approved by the Institutional Animal Care and Use Committee of the Seoul National University Bundang Hospital (SNUBH).

Small Animal PET/CT Imaging Protocol. Five rats (227.98 ± 13.8 g) were used for brain PET imaging at 4 days after LPS injection. Before the scan, the rats were anesthetized with 5% isoflurane and thereafter sustained with 1−2% isoflurane in a 7:3 mixture of N_2/O_2. PET imaging was performed in a dedicated small animal PET/CT (NanoPET/CT, Bioscan, Inc., Washington, DC, U.S.), with a 10 cm axial field of view (FOV) and a 12 cm transaxial FOV. This scanner yields a reconstructed PET spatial resolution of 1.2 mm full-width at half-maximum at the center of the field of view. A CT scan of the head as a transmission map for attenuation correction was studied prior to the emission study. PET acquisition in the list mode was concomitantly started with the intravenous injection of either [^{11}C]PBR28 or [^{18}F]-fluoromethyl-PBR28 and was performed for 90 min. The first exam was studied with [^{11}C]PBR28, and the second exam followed 3.5 h later with [^{18}F]fluoromethyl-PBR28 in same rat models (Figure 2). At the end of each study, the list-mode data

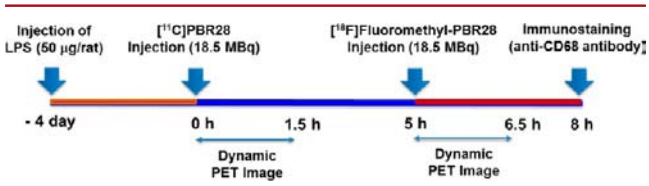

Figure 2. microPET imaging protocol.

were sorted into a dynamic scan consisting of 64 frames. The acquired images were reconstructed by a 3-D Adjoint Monte Carlo method, combined with scatter and random corrections. Reconstructed voxel values in each frame are reported in units of kBq/cc, corrected for radioactive decay to the time of injection, and the voxel dimensions were 0.4 × 0.4 × 0.4 mm^3. The voxel values were then converted to units of percentage injected dose per cubic centimeter (cc) of brain tissue.

Image Analysis. Analysis of the PET images was performed using PMOD software v.3.1 (PMOD Technologies Ltd., Zurich, Switzerland). The volume of interest (VOI) with a 2 mm radius was delineated in the ipsilateral lesioned striatum by the intensely visualized region in the summed image of all the frames. The VOI of the lesion was copied and symmetrically plated into the contralateral striatum. The radiotracer uptake in each ROI was estimated as the percentage of the injection dose per cubic centimeter (%ID/cc). The time activity curve (TAC) representing the variation in radioligand concentration according to the time course was estimated for the ipsilateral/contralateral striatum.

Immunohistochemical Study. Immunohistochemical staining was performed on neuroinflammatory rats (222.7 ± 5.9 g) just after the end of the PET study using [^{18}F]-fluoromethyl-PBR28. The rats were transcardially perfused under pentobarbital anesthesia (50 mg/kg, intraperitoneally) with 5 mL of phosphate buffered saline (PBS), followed by 20 mL of 4% paraformaldehyde (pH 7.4). The brains were quickly removed, postfixed in the same fixative overnight at 4 °C, and then embedded in 30% sucrose solution for the following 3 days. Next, the brains were slowly frozen and maintained at −20 °C and sliced at 40 μm at the coronal section of the LPS-lesioned striatum. The sections were directly mounted onto slides and blocked with 4.5% normal goat serum and 0.1% Triton 100 in PBS (60 min at room temperature). Next, the slides were incubated with the primary antibody, mouse anti-CD68 (1:100; Serotec, Oxford, UK), overnight at 4 °C, and detected using the HRP-conjugated goat antimouse IgG antibody (1:500; Vector Laboratories, Burlingame, CA). Antibody reactivity was visualized using the Vectastain ABC Elite Kit (Vector Laboratories, Burlingame, CA) and the diaminobenzidine (DAB) Zytomed kit (DAB057; Zytomed Systems, Berlin, Germany). After staining, a fluorescence microscope (Axio Observer, Zeiss, Germany) with Image-Pro Plus 7.0 software was used to histologically quantify the density ratio of CD68-positive activated microglia in the ipsilateral and contralateral striatum.

dx.doi.org/10.1021/bc400556h | *Bioconjugate Chem.* 2014, 25, 442−450

Blocking and Displacement Study. For the displacement PET study of [^{18}F]fluoromethyl-PBR28, PBR28 (5 mg/kg intravenously) was administered 30 min after the injection of [^{18}F]fluoromethyl-PBR28 (n = 4; 222.7 ± 5.9 g).[25] In blocking studies for specificity and selectivity, [^{18}F]fluoromethyl-PBR28 involved coinjection with PK11195 (10 mg/kg intravenously), compound **1** (5 mg/kg intravenously), and flumazenil (5 mg/kg intravenously) were performed.

Metabolism Study in Rat Brain and Plasma. [^{18}F]-Fluoromethyl-PBR28 (approximately 37 MBq, 0.5 mL of 5% EtOH:saline) was intravenously injected into the neuroinflammation rat models via a tail vein. After 30 and 60 min, the rat was sacrificed and samples of the brain were collected. The brain samples were homogenized in 2 mL of 50% CH_3CN-PBS (3 times) in a commercial blender for 3 min and centrifuged at 3500 rpm for 5 min at 4 °C. The resulting supernatant was filtered through a 0.45 μm GH Polypro (GHP) membrane Disc filter. The samples were analyzed with an authentic compound by HPLC (Waters, Xterra RP-18, 10 × 250 mm) with a guard column (10 × 10 mm); eluant: 45% CH_3CN/H_2O; flow rate: 3 mL/min). The extraction ratios from the brain homogenate after 30 and 60 min postinjection into the rat were approximately 92% and 89%, respectively. The blood samples (2, 5, 15, 60, and 90 min postinjection, n = 3) was centrifuged at 15 000 rpm for 1 min at 4 °C to separate the plasma (0.3 mL), which was collected in a test tube containing CH_3CN (0.5 mL) and a solution of the authentic fluoromethyl-PBR28 (1.0 mg/2.0 mL of CH_3CN, 50 μL) was added. After the tube was vortexed for 15 s and centrifuged at 15 000 rpm for 2 min for deproteinization, the supernatant was collected. The resulting supernatant was filtered through a 0.45 μm GH Polypro (GHP) membrane Disc filter. The samples were analyzed by HPLC as described above. The extraction efficiency of the total radioactivity was 78.5 ± 5.9%.

Statistical Analysis. Data are expressed as the mean ± standard deviation and analyzed using the Mann−Whitney test. The statistical significance of the p values was defined as <0.05. The statistical analysis was performed using SPSS 12 (SPSS, Inc., Chicago, IL, USA).

RESULTS AND DISCUSSION

For the preparation of the triazolium triflate precursor for the one-step labeling with fluorine-18, desmethyl PBR28 (**6**) was prepared according to the procedure described in the literature with little modifications.[26] The triazolium triflate-PBR28 (**7**) was synthesized via alkylation between desmethyl PBR28 and 1-(chloromethyl)-3-methyl-4-phenyl-1*H*-1,2,3-triazol-3-ium triflate (**5**), and authentic compound, fluoromethyl-PBR28 (**1**) was easily obtained from the reaction of tetra-*n*-butylammonium fluoride (TBAF)-3H_2O with the triazolium triflate-PBR28 precursor (Scheme 1).

The radiosynthesis of [^{18}F]**1** was investigated from **7** by nucleophilic aliphatic substitution with the TBA[^{18}F]F complex in one-step reaction under different solvents (Table 1). Among the various conditions investigated for fluorine-18 labeling, aprotic polar solvents, such as acetonitrile or *N*,*N*-dimethylformamide (DMF), which are well-known as suitable S_N2 reaction media, were not efficient for fluorine-18 incorporation into [^{18}F]**1**, resulting in less than 1% of radiochemical yield, unlike the preparation of the authentic compound **1**. This low yield is irrelevant compared to the increase of the precursor amounts or the increase in reaction temperature from 60 to 150 °C. The cause of this low yield was that the precursor decomposed

Table 1. Radiosynthesis of [^{18}F]1 under Various Conditions[a]

entry	solvent	time (min)	temp. (°C)	RCY (%)[b]
1	CH_3CN	10	60	<1
2	CH_3CN	10	80	<1
3	CH_3CN	10	120	<1
4	DMF	10	150	<1
5	t-BuOH	10	120	64 ± 4.2[c]
6	t-BuOH	15	120	58 ± 4.7[c]
7	*t*-BuOH:CH_3CN (4:1)	10	120	45 ± 6.3[c]
8[d]	t-BuOH	10	120	56 ± 5.5[c]

[a]The reaction was carried out using 0.8 equiv of $TBAHCO_3$ relative to the precursor (2.3 mg) in 0.4 mL of solvent. [b]The radiochemical yield (RCY) was determined by radio-TLC (n = 3 or 4). [c]n = 11. [d]Amount of precursor: 4.5 mg.

under the basic conditions during fluoride-18 incorporation. In fact, the precursor was not detected in the reaction mixture after radiofluorination when checked by UV at 254 nm in TLC. A recent study demonstrated that nucleophilic aliphatic fluorination via the S_N2 mechanism is dramatically accelerated in tertiary alcohol solvents compared to that in aprotic polar solvents.[27] Using this strategy, the labeling yield of [^{18}F]**1** approached 64% when performed in *tert*-butanol as reaction solvent at 120 °C for 10 min. Although a 10 min reaction was sufficient, the reaction time was extended to 15 min because the radiochemical yield slightly decreased. Increasing the amount of precursor from 2.3 mg to 4.5 mg (entry 5 versus entry 8) was not significant in this experiment. It could be considered that this slightly low radiochemical yields might be the result of the stability of the triazolium triflate precursor under more basic condition because of the increased base as equivalent of precursor. Changing the reaction solvent to one such as *tert*-butanol:CH_3CN (4:1), resulted in a lower yield of approximately 45%; moreover, the purification of [^{18}F]**1** from the reaction mixtures was also difficult because of the many impurities, resulting in low specific activity. By using the optimized conditions described above, the radiochemical yield of the final formulated [^{18}F]**1** product was 35.8 ± 3.2% (n = 11, decay corrected) within a synthesis time of 55 min, including HPLC purification of the reaction mixture (Figure S1). The specific activity of [^{18}F]**1** at the end of the synthesis ranged from 220−340 GBq/μmol. Co-injection of the radioactive product with the authentic standard of **1** under different conditions further established the identity of [^{18}F]**1** (Figure S2). The formulated radiotracer displayed no radiolysis for at least 120 min postformulation and required no stabilizing agents such as ascorbate. To compare TSPO specificity between [^{18}F]**1** and [^{11}C]**2** ([^{11}C]PBR28), [^{11}C]**2** was efficiently and rapidly synthesized from **6** and [^{11}C]CH_3OTf using the FX C-pro module (Figure S3). The isolated radiochemical yield was 20−30% (decay corrected), to yield approximately 3.7−4.5 GBq per batch with 277 ± 101 GBq/μmol of specific activity.

The affinity (IC_{50}) was measured by competition with [^{3}H]PK11195 in a membrane of human leukocytes.[28] The binding affinity and the partition coefficient (log D) of fluoromethyl-PBR28 are similar to those of PBR28 (IC_{50} = 8.28 ± 1.79 nM versus 8.07 ± 1.40 nM; Figure 1). These biological similarities may be due to the bioisostere effect of monovalent atoms in the -OCH_2F and -OCH_2H group.[29] The in vitro stability of [^{18}F]**1** in human serum demonstrated that

dx.doi.org/10.1021/bc400556h | *Bioconjugate Chem.* 2014, 25, 442−450

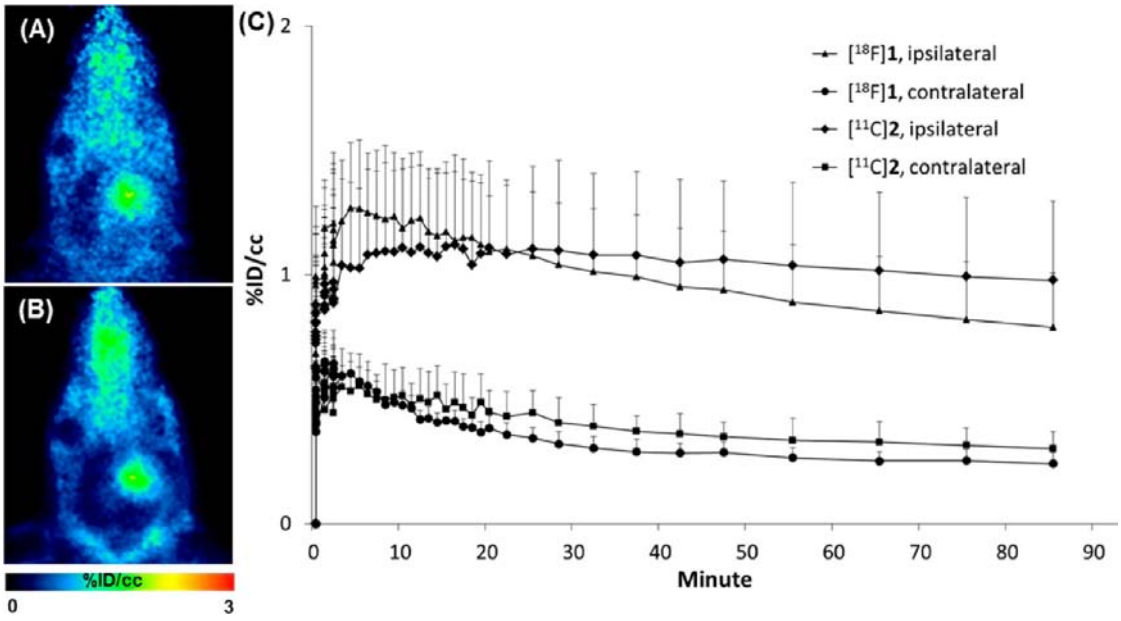

Figure 3. Brain PET images and time-activity curves of two radiotracers in a rat LPS model of neuroinflammation (n = 5). PET images shown are summed images between 30 and 50 min after injection of [^{11}C]**2** (A) and [^{18}F]**1** (B).

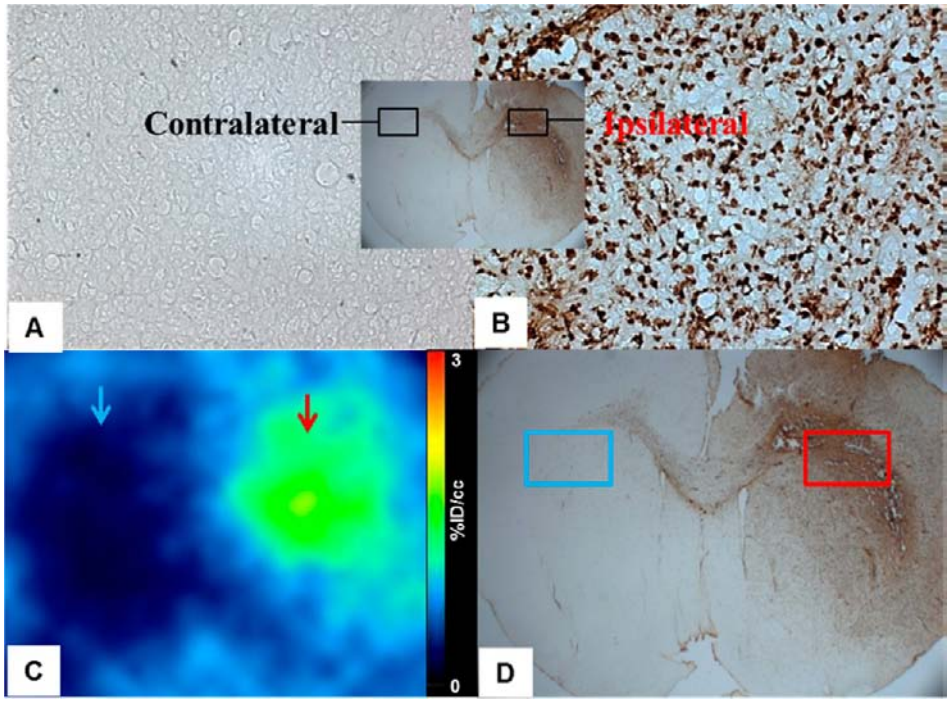

Figure 4. Immunohistochemical staining (anti-CD68; Serotec, Oxford, UK) of the ipsilateral (A: 20×) and contralateral area (B: 20×) in the neuroinflammatory rat model. The 90 min summed PET image using [^{18}F]fluoromethyl-PBR28 (C) and the image of the immunohistochemically stained rat brain (D; anti-CD68; Serotec, Oxford, UK) of the neuroinflammatory rat model.

the radioactive parent remained over 99% for 4 h (Figure S4). This high stability indicated that [^{18}F]**1** was sufficiently stable for use in further in vivo biological studies.

To further examine the potential of [^{18}F]**1**, it was compared directly to [^{11}C]**2** in a rat lipopolysaccharide (LPS) model of neuroinflammation using sequential scans of [^{11}C]**2** and [^{18}F]**1** (Figure 3). The time-activity curves of the radioactivity of both radioligands between the ipsilateral and contralateral area were compared to identify the pharmacokinetic properties in the rat LPS model.

[^{18}F]**1** and [^{11}C]**2** had slightly different pharmacokinetic profiles (Figure 2C). While the uptake of [^{11}C]**2** in the ipsilateral area approached a steady state at nearly 20 min postinjection, [^{18}F]**1** rapidly peaked at around 4.5 min postinjection and then slowly declined in the remainder of the scan (linear regression slope = [^{18}F]**1** with −0.0063 ± 0.0026; [^{11}C]**2** with −0.0017 ± 0.0013; p = 0.016). In addition, the clearance of [^{18}F]**1** in the contralateral area was faster than that of [^{11}C]**2** (linear regression slope = [^{18}F]**1** with −0.0054 ± 0.0006; [^{11}C]**2** with −0.0032 ± 0.0014; p = 0.032). The highest

dx.doi.org/10.1021/bc400556h | *Bioconjugate Chem.* 2014, 25, 442−450

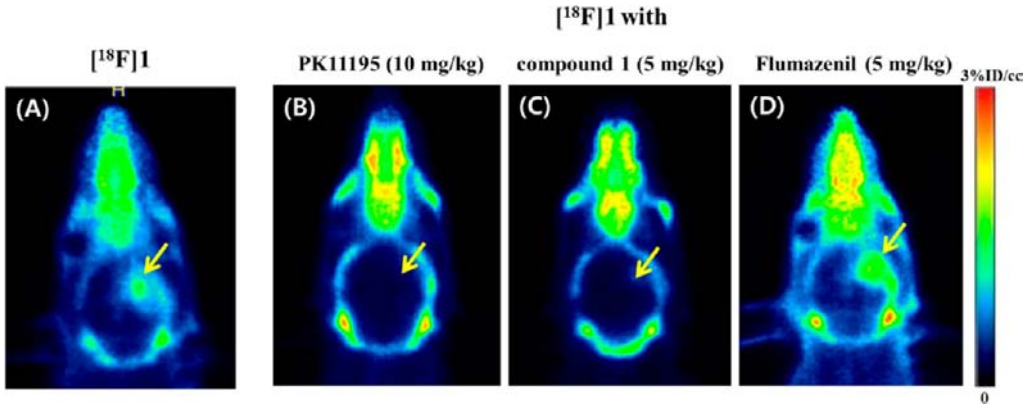

Figure 5. PET images (%ID/cc, horizontal plane) of [^{18}F]**1** in the neuroinflammatory rat model. Summed images (0–90 min) of [^{18}F]**1** in control study (A) and displacement by PK11195 (B, 10 mg/kg), compound 1 (C, 5 mg/kg), or flumazenil (D, 5 mg/kg).

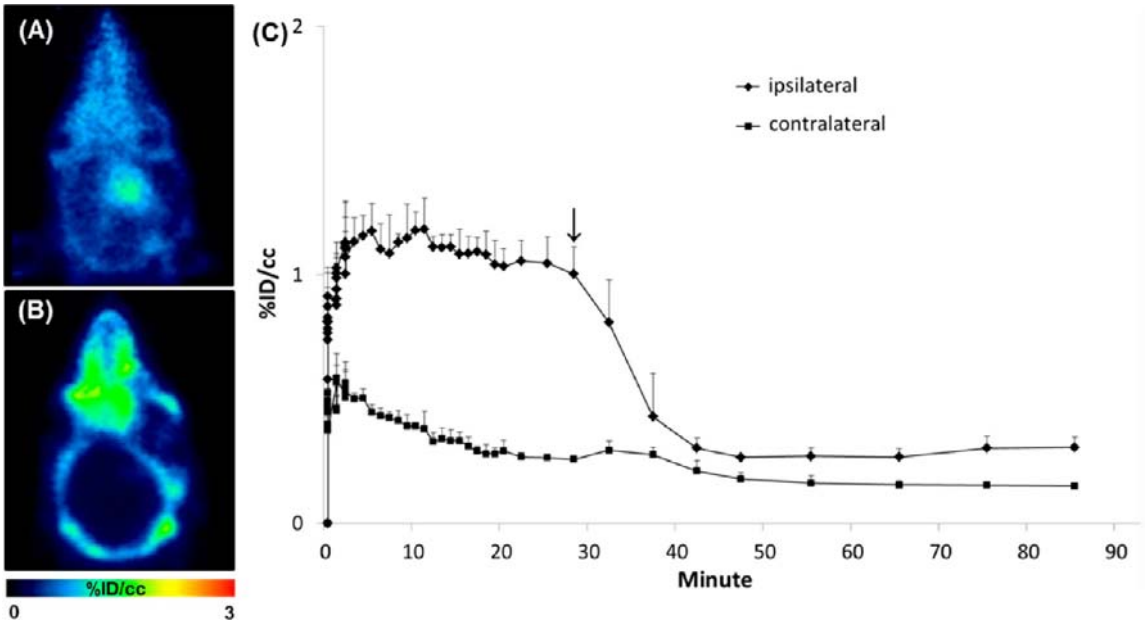

Figure 6. Brain PET images (A and B) and time-activity curves (C) of [^{18}F]**1** in the displacement study with PBR28 (n = 4). The injection of unlabeled PBR28 was done at 30 min. PET images shown are summed images between 0 and 30 min after injection of [^{18}F]**1** (A) and between 30 and 90 min (B).

uptake ratio of [^{18}F]**1** between the ipsilateral area and the contralateral area displayed in a shorter period of time than [^{11}C]**2** ([^{18}F]**1** at 35 min with 3.4 times; [^{11}C]**2** at 85 min with 3.2 times).

In all of the rats used for sequential PET scans, the microglial activation was checked by immunohistochemical CD68 staining. The selective PET images of both radioligands showed a high density of CD68-positive activated microglia in the ipsilateral area compared to the contralateral area (Figure 4).

To determine whether the radioactivity accumulation in the LPS-induced inflammation is specific and selective for TSPO, we performed blocking experiments in which the rat LPS model was coinjected with PK11195 (10 mg/kg), cold authentic compound **1** (5 mg/kg), and flumazenil (5 mg/kg) with [^{18}F]**1**, respectively (Figure 5). Compared with the baseline study of [^{18}F]**1**, the uptake of the ipsilateral area significantly decreased after coinjection with PK11195 or **1**, for which the relative uptake reductions were 67% and 71%, respectively. In addition, flumazenil, which binds to the central benzodiazepine receptor, did not intercept the uptake of [^{18}F]**1** in the ipsilateral area of the rat LPS model.

Moreover, the study of the displacement of [^{18}F]**1** was performed by injecting an excess of PBR28 (5 mg/kg) 30 min postinjection, when the highest uptake radio of [^{18}F]**1** between the ipsilateral and contralateral area appeared (Figure 6). The initial uptake of [^{18}F]**1** was similar to the baseline study. After the injection of PBR28, the radioactivity of the ipsilateral area was rapidly displaced and reached a similar level to that of the contralateral area. While the uptake of the ipsilateral area was 1.00% ID/cc 30 min after the injection of [^{18}F]**1**, it decreased to 0.27% ID/cc 50 min after the injection of 1.2 mg of unlabeled PBR28. Our blocking and displacement studies indicate that the inflammatory lesion images of [^{18}F]**1** are selectively mediated by TSPO.

In an in vivo stability study in the rat LPS model, intact [^{18}F]**1** and metabolites were measured by HPLC (Figure S5). The radioactive parent remained 98.3% and 97.8% of the initial value at 30 and 60 min after the injection, respectively. No other major metabolites were observed at the end of the

dx.doi.org/10.1021/bc400556h | *Bioconjugate Chem.* 2014, 25, 442–450

examination, except for approximately 2% of an unidentified molecule. In the plasma fraction, two radioactive metabolites appeared in the HPLC profile. The initial percentage of intact [^{18}F]**1** in the plasma (69.0 ± 4.7% at 2 min postinjection) was rapidly degraded to 26.8 ± 4.1% at 5 min postinjection and slowly declined for the remainder of the study (Table S1, Figures S6 and S7). The percentage of metabolite **1** increased as much as that of the broken intact. A small amount of the unidentified radioactive metabolite **2** was detected in the plasma, but it rapidly disappeared after 15 min postinjection. Despite the relative low stability of [^{18}F]**1** in rat plasma and the appearance of bone images at late scan time in small animal model, in vitro stability assay in human serum was shown to be quite stable. This demonstrates that [^{18}F]**1** is expected to maintain sufficient stability in humans.

In summary, we successfully developed a promising TSPO-targeted ligand which was introduced as the [^{18}F]fluoromethyl moiety, [^{18}F]**1**, for TSPO PET imaging of neuroinflammation. Our radiofluorination of the fluoromethoxy group from a triazolium triflate precursor proceeds efficiently and rapidly for [^{18}F]fluoromethyl-PBR28. Although [^{18}F]fluoromethyl-PBR28 and [^{11}C]PBR28 have similar in vitro biological properties (i.e., IC_{50} and log *D*), the two radiotracers showed slightly different pharmacokinetic patterns in the in vivo PET study, which may be due to the different monovalent atom. Comparatively, [^{18}F]fluoromethyl-PBR28 displays the inflammatory lesion with an excellent target-to-background ratio at early imaging time compared to [^{11}C]PBR28, without a noticeable skull image. The specific TSPO-binding uptake and metabolism studies presented here suggest that [^{18}F]fluoromethyl-PBR28 has potential as a neuroinflammation PET imaging agent in the field of brain disorders. In conclusion, we have described that the preparation of [^{18}F]fluoromethyl ether group should enable the facile preparation of a number of biologically active molecules bearing *O*-fluoromethyl groups, and demonstrated [^{18}F]fluoromethyl-PBR28, for which fluorine has effectively replaced hydrogen and retained comparable TSPO activity, albeit with different properties. The novel direct radiofluorination method for the introduction of the [^{18}F]-fluoromethyl moiety could be applied to various fluorine-18 labeled radiopharmaceuticals.

■ ASSOCIATED CONTENT

Supporting Information

Byung Seok Moon and Bom Sahn Kim contributed equally to this study. This material is available free of charge via the Internet at http://pubs.acs.org.

■ AUTHOR INFORMATION

Corresponding Authors

*Phone: +82 31 787 2957. Fax: +82 31 787 4072. E-mail: leebc@snu.ac.kr (B.C.L.).

*Phone: +82 31 787 7671. Fax: +82 31 787 4018. E-mail: kse@snu.ac.kr (S.E.K.).

*Phone: +82 505 860 7686. Fax: +82 2 3010 8516. E-mail: dychi@sogang.ac.kr (D.Y.C.).

Notes

The authors declare no competing financial interest.

■ ACKNOWLEDGMENTS

This study was supported by grants (HI09C-1444-010013, 2012R1A1A2005887, 2012K001486, 20090078370, and HI12C-0035-030013) of South Korea.

■ REFERENCES

(1) Banati, R. B., Egensperger, R., Maassen, A., Hager, G., Kreutzberg, G. W., and Graeber, M. B. (2004) Mitochondria in activated microglia in vitro. *J. Neurocytol. 33*, 535−41.

(2) Venneti, S., Lopresti, B. J., and Wiley, C. A. (2006) The peripheral benzodiazepine receptor (Translocator protein 18 kDa) in microglia: From pathology to imaging. *Prog. Neurobiol. 80*, 308−22.

(3) Diorio, D., Welner, S. A., Butterworth, R. F., Meaney, M. J., and Suranyi-Cadotte, B. E. (1991) Peripheral benzodiazepine binding sites in Alzheimer's disease frontal and temporal cortex. *Neurobiol. Aging 12*, 255−8.

(4) Messmer, K., and Reynolds, G. P. (1998) Increased peripheral benzodiazepine binding sites in the brain of patients with Huntington's disease. *Neurosci. Lett. 241*, 53−6.

(5) Banati, R. B., Newcombe, J., Gunn, R. N., Cagnin, A., Turkheimer, F., Heppner, F., Price, G., Wegner, F., Giovannoni, G., Miller, D. H., Perkin, G. D., Smith, T., Hewson, A. K., Bydder, G., Kreutzberg, G. W., Jones, T., Cuzner, M. L., and Myers, R. (2000) The peripheral benzodiazepine binding site in the brain in multiple sclerosis: quantitative in vivo imaging of microglia as a measure of disease activity. *Brain 123*, 2321−37.

(6) Imaizumi, M., Kim, H. J., Zoghbi, S. S., Briard, E., Hong, J., Musachio, J. L., Ruetzler, C., Chuang, D. M., Pike, V. W., Innis, R. B., and Fujita, M. (2007) PET imaging with [^{11}C]PBR28 can localize and quantify upregulated peripheral benzodiazepine receptors associated with cerebral ischemia in rat. *Neurosci. Lett. 411*, 200−5.

(7) Cagnin, A., Kassiou, M., Meikle, S. R., and Banati, R. B. (2007) Positron emission tomography imaging of neuroinflammation. *Neurotherapeutics 4*, 443−52.

(8) Shah, F., Hume, S. P., Pike, V. W., Ashworth, S., and McDermott, J. (1994) Synthesis of the enantiomers of [*N*-methyl-^{11}C]PK11195 and comparison of their behaviours as radioligands for PK binding sites in rats. *Nucl. Med. Biol. 21*, 573−81.

(9) Petit-Taboué, M. C., Baron, J. C., Barré, L., Travère, J. M., Speckel, D., Camsonne, R., and MacKenzie, E. T. (1991) Brain kinetics and specific binding of [^{11}C]PK 11195 to omega 3 sites in baboons: positron emission tomography study. *Eur. J. Pharmacol. 200*, 347−51.

(10) Doorduin, J., Klein, H. C., de Jong, J. R., Dierckx, R. A., and de Vries, E. F. (2010) Evaluation of [^{11}C]DAA1106 for imaging and quantification of neuroinflammation in a rat model of herpes encephalitis. *Nucl. Med. Biol. 37*, 9−15.

(11) Zhang, M. R., Kida, T., Noguchi, J., Furutsuka, K., Maeda, J., Suhara, T., and Suzuki, K. (2003) [^{11}C]DAA1106: radiosynthesis and in vivo binding to peripheral benzodiazepine receptors in mouse brain. *Nucl. Med. Biol. 30*, 513−9.

(12) Chauveau, F., Boutin, H., Van Camp, N., Dollé, F., and Tavitian, B. (2008) Nuclear imaging of neuroinflammation: a comprehensive review of [^{11}C]PK11195 challengers. *Eur. J. Nucl. Med. Mol. Imaging 35*, 2304−19.

(13) Imaizumi, M., Briard, E., Zoghbi, S. S., Gourley, J. P., Hong, J., Fujimura, Y., Pike, V. W., Innis, R. B., and Fujita, M. (2008) Brain and whole-body imaging in nonhuman primates of [^{11}C]PBR28, a promising PET radioligand for peripheral benzodiazepine receptors. *NeuroImage 39*, 1289−98.

(14) Schou, M., Halldin, C., Sóvágó, J., Pike, V. W., Hall, H., Gulyás, B., Mozley, P. D., Dobson, D., Shchukin, E., Innis, R. B., and Farde, L. (2004) PET evaluation of novel radiofluorinated reboxetine analogs as norepinephrine transporter probes in the monkey brain. *Synapse 53*, 57−67.

(15) Donohue, S. R., Krushinski, J. H., Pike, V. W., Chernet, E., Phebus, L., Chesterfield, A. K., Felder, C. C., Halldin, C., and Schaus, J. M. (2008) Synthesis, ex vivo evaluation, and radiolabeling of potent

1,5-diphenylpyrrolidin-2-one cannabinoid subtype-1 receptor ligands as candidates for in vivo imaging. *J. Med. Chem. 51*, 5833−42.
(16) Iwata, R., Pascali, C., Bogni, A., Furumoto, S., Terasaki, K., and Yanai, K. (2002) [^{18}F]Fluoromethyl triflate, a novel and reactive [^{18}F]fluoromethylating agent: preparation and application to the on-column preparation of [^{18}F]fluorocholine. *Appl. Radiat. Isot. 57*, 347−52.
(17) Park, C., Lee, B. S., and Chi, D. Y. (2013) High efficiency synthesis of F-18 fluoromethyl ethers: an attractive alternative for C-11 methyl groups in positron emission tomography radiopharmaceuticals. *Org. Lett. 15*, 4346−9.
(18) Kalisiak, J., Sharpless, K. B., and Fokin, V. V. (2008) Efficient synthesis of 2-substituted-1,2,3-triazoles. *Org. Lett. 10*, 3171−4.
(19) Park, C., Kang, H., Lee, S. Y., Lee, J. H., Lee, B. S., and Chi, D. Y. (2013) Efficient synthesis of O-[^{18}F]fluoromethyltyrosine ([^{18}F]FMT). *J. Labelled Compds Radiopharm. 56*, S72.
(20) Briard, E., Zoghbi, S. S., Imaizumi, M., Gourley, J. P., Shetty, H. U., Hong, J., Cropley, V., Fujita, M., Innis, R. B., and Pike, V. W. (2008) Synthesis and evaluation in monkey of two sensitive ^{11}C-labeled aryloxyanilide ligands for imaging brain peripheral benzodiazepine receptors in vivo. *J. Med. Chem. 51*, 17−30.
(21) Hoareau, R., Shao, X., Henderson, B. D., and Scott, P. J. (2012) Fully automated radiosynthesis of [^{11}C]PBR28, a radiopharmaceutical for the translocator protein (TSPO) 18 kDa, using a GE TRACERlab FXC-Pro. *Appl. Radiat. Isot. 70*, 1779−83.
(22) Wang, M., Yoder, K. K., Gao, M., Mock, B. H., Xu, X. M., Saykin, A. J., Hutchins, G. D., Zheng, Q. H., Hutchins, G. D., and Zheng, Q.-H. (2009) Fully automated synthesis and initial PET evaluation of [^{11}C]PBR28. *Bioorg. Med. Chem. Lett. 19*, 5636−9.
(23) Kreisl, W. C., Fujita, M., Fujimura, Y., Kimura, N., Jenko, K. J., Kannan, P., Hong, J., Morse, C. L., Zoghbi, S. S., Gladding, R. L., Jacobson, S., Oh, U., Pike, V. W., and Innis, R. B. (2010) Comparison of [^{11}C]-(R)-PK11195 and [^{11}C]PBR28, two radioligands for translocator protein (18 kDa) in human and monkey: Implications for positron emission tomographic imaging of this inflammation biomarker. *Neuroimage 49*, 2924−32.
(24) Chauveau, F., Van Camp, N., Dollé, F., Kuhnast, B., Hinnen, F., Damont, A., Boutin, H., James, M., Kassiou, M., and Tavitian, B. (2009) Comparative evaluation of the translocator protein radioligands ^{11}C-DPA-713, ^{18}F-DPA-714, and ^{11}C-PK11195 in a rat model of acute neuroinflammation. *J. Nucl. Med. 50*, 468−76.
(25) Van Camp, N., Boisgard, R., Kuhnast, B., Thézé, B., Viel, T., Grégoire, M. C., Chauveau, F., Boutin, H., Katsifis, A., Dollé, F., and Tavitian, B. (2010) In vivo imaging of neuroinflammation: a comparative study between [^{18}F]PBR111, [^{11}C]CLINME and [^{11}C]-PK11195 in an acute rodent model. *Eur. J. Nucl. Med. Mol. Imaging 37*, 962−72.
(26) Wilson, A. A., Garcia, A., Parkes, J., McCormick, P., Stephenson, K. A., Houle, S., and Vasdev, N. (2008) Radiosynthesis and initial evaluation of [^{18}F]-FEPPA for PET imaging of peripheral benzodiazepine receptors. *Nucl. Med. Biol. 35*, 305−14.
(27) Kim, D. W., Jeong, H. J., Lim, S. T., Sohn, M. H., Katzenellenbogen, J. A., and Chi, D. Y. (2008) Facile nucleophilic fluorination reactions using *tert*-alcohols as a reaction medium: significantly enhanced reactivity of alkali metal fluorides and improved selectivity. *J. Org. Chem. 73*, 957−62.
(28) Ferrarese, C., Appollonio, I., Frigo, M., Perego, M., Piolti, R., Trabucchi, M., and Frattola, L. (1990) Decreased density of benzodiazepine receptors in lymphocytes of anxious patients: reversal after chronic diazepam treatment. *Acta Psychiatr. Scand. 82*, 169−73.
(29) Patani, G. A., and LaVoie, E. J. (1996) Bioisosterism: a rational approach in drug design. *Chem. Rev. 96*, 3147−716.